Molybdate- and Tungstate-Exchanged Layered Double Hydroxides as Catalysts for $^1O_2$ Formation: Characterization of Reactive Oxygen Species and a Critical Evaluation of $^1O_2$ Detection Methods

Bert F. Sels, Dirk E. De Vos, Piet J. Grobet, Frédéric Pierard,† F. Kirsch-De Mesmaeker,† and Pierre A. Jacobs*

Centre for Surface Chemistry and Catalysis, Katholieke Universiteit Leuven, Kardinaal Mercierlaan 92, 3001 Heverlee, Belgium

Received: June 30, 1999; In Final Form: September 18, 1999

Layered double hydroxides (LDHs) with the formula $[Mg_{0.7}Al_{0.3}(OH)_2](NO_3)_{0.3}$ were partially exchanged with MoO_4^{2-} and WO_4^{2-} and were used as heterogeneous catalysts for the decomposition of H_2O_2 into singlet molecular oxygen ($^1O_2$). The oxometalate anions are present on the LDH as monomeric, tetrahedral MO_4^{2-} anions. With LDH−MoO_4^{2-} and H_2O_2, $^1O_2$ is by far the prevailing reactive oxygen species. EPR trapping detected a minor amount of free $OH^\bullet$ radicals, but these do not appreciably contribute to product formation in olefin oxygenation. LDH−WO_4^{2-} transforms H_2O_2 into $^1O_2$ about 4 times slower than the Mo catalyst, and additionally effects mono-oxygen transfer to electron-rich substrates such as amines and olefins. Only for alkenes with very low β values, the Schenck hydroperoxidation dominates over the epoxidation in the W-catalyzed reactions. While most tests for $^1O_2$ detection were designed for photosensitized reactions, the applicability of these methods to dark catalytic reactions is not always clear. Therefore, a series of common $^1O_2$ detection methods was critically evaluated in the LDH−WO_4^{2-} or LDH−MoO_4^{2-} + H_2O_2 reactions. Isomer distributions in the olefin hydroperoxidation and detection of NIR luminescence are the most reliable and sensitive methods. Quenching or trapping methods that involve amines should not be used when the catalyst also effects mono-oxygenation.

Introduction

Dioxygen in its first excited singlet state ($^1\Delta_g$) is a regio- and stereoselective reagent for the preparation of hydroperoxides, allylic alcohols, endoperoxides, diepoxides, or even for ring-opening reactions.[1] Practical use requires the availability of singlet oxygen ($^1O_2$) sources that can generate high $^1O_2$ fluxes without causing side reactions, such as light-induced radical reactions or chlorinations in the case of the Kasha−Khan reagent (OCl^-/H_2O_2). A promising alternative is therefore the controlled, nonradical disproportionation of H_2O_2,

$$2H_2O_2 \rightarrow 2H_2O + {}^1O_2 \qquad (1)$$

The acceleration of this reaction by a series of dissolved mineral compounds has been documented in much detail, and procedures for homogeneous catalytic oxygenation have been proposed.[2,3] We have recently reported that the use of a molybdate-exchanged layered double hydroxide (LDH) as a catalyst for reaction 1 has several advantages.[4] First, the LDH with its high anion exchange capacity has a strong affinity for the molybdate, which ensures true heterogeneity of the molybdate.[5] Second, as high substrate concentrations can be used in a salt-free reaction solvent, substrate oxygenation is favored over solvent quenching of $^1O_2$. Finally, heterogeneous catalysis has obvious advantages for workup and catalyst reuse.

The present full paper presents detailed proof of the generation of $^1O_2$ from H_2O_2 in the presence of LDH−MoO_4^{2-} and LDH−WO_4^{2-}. First, in a thorough characterization of the materials, it will be demonstrated that the metal speciation on these LDHs is different from that on pillared LDHs, which have been used in epoxidation catalysis.[6] Next, the MoO_4^{2-} and WO_4^{2-} exchanged LDHs are compared in their ability to transform H_2O_2 into $^1O_2$ or other reactive oxygen species. Typical tests for detection of $^1O_2$ include trapping experiments, spectroscopy, and reactions with organic substrates, such as mono-olefins, dienes, or aromatics. Such tests are frequently employed in the dye-sensitized generation of $^1O_2$ but have rarely been applied in heterogeneously catalyzed $^1O_2$ generation. Therefore, the results with the LDH catalysts will be used to critically evaluate the scope or the limitations of the various methods for $^1O_2$ detection.

Experimental Section

Materials. α-Terpinene, rubrene, 1,3-diphenylisobenzofuran, *N-tert*-butyl-α-phenylnitrone, 2,6-di-*tert*-butylphenol, cyclohexene, $Mg(NO_3)_2 \cdot 6H_2O$, and $Na_2WO_4 \cdot 2H_2O$ were purchased from Acros. 1,4-Dimethylnaphthalene, 2,2,6,6-tetramethylpiperidine, TEMPO, 1-methylcyclopentene, 1-methylcyclohexene, cyclopentene, 2,3,4-trimethyl-2-pentene, 2,3-dimethyl-2-butene, $Na_2MoO_4 \cdot 2H_2O$, and KO_2 were purchased from Aldrich. 2-Methyl-2-pentene and $Al(NO_3)_3 \cdot 9H_2O$ were from Fluka, 2-methyl-2-butene from Alfa, and 1-methylcycloheptene from ICN. All products were of the highest commercial grade and were used as such. Only DABCO (Fluka) was recrystallized twice from acetone before use.

* Corresponding author. Phone: 32 16 32 1465. Fax: 32 16 32 1998. E-mail: pierre.jacobs@agr.kuleuven.ac.be.

† Physical Organic Chemistry CP 160/08, UL Bruxelles, 1000 Bruxelles, Belgium.

10.1021/jp992236z CCC: $18.00
Published on Web 11/30/1999

Catalyst Preparation. LDH preparation was based on literature procedures.[5] LDH−NO_3^- was prepared by coprecipitation of Mg and Al nitrate salts. In a 1 L three-neck round-bottom flask, 100 mL of deionized and boiled water was brought to pH 10 ± 0.2 with 1 N NaOH. Next, 120 mL of 0.3 M $Al(NO_3)_3 \cdot 6H_2O$ and 120 mL of 0.7 M $Mg(NO_3)_2 \cdot 6H_2O$ were simultaneously added (60 mL/h for each) under N_2 atmosphere at room temperature. The pH of the slurry was maintained at 10 ± 0.2 by addition of 1 M NaOH. After addition of the nitrate salts, the suspension was stirred for 24 h at ambient temperature. The white precipitate formed was washed, centrifuged four times, and dried by lyophilization (yield ∼90% based on Mg added). For ion exchange, 1.5 g of the LDH−NO_3^- was suspended in 150 mL of a 1.875 mM aqueous $Na_2WO_4 \cdot 2H_2O$ or $Na_2MoO_4 \cdot 2H_2O$ solution and stirred for 12 h at ambient temperature under N_2 atmosphere. The pH of the final suspension was 9.3 ± 0.2. The final solid products (LDH−MoO_4^{2-} and LDH−WO_4^{2-}) were obtained by repeated centrifugation−washing cycles, eventually followed by lyophilization.

Reaction Procedures. LDH−MoO_4^{2-} or LDH−WO_4^{2-} catalysts contain 0.187 mmol Mo or W per gram of lyophilized and ambient air rehydrated solid. Homogeneous reactions were performed with $Na_2MoO_4 \cdot 2H_2O$ or $Na_2WO_4 \cdot 2H_2O$ in 0.01 N NaOH in a 15:85 volumetric ratio of water and methanol. Comparisons between heterogeneous and homogeneous catalysts were made for equal total concentrations of Mo or W. Reactions were generally performed with stirring at room temperature. Yields are calculated as (moles of desired product formed)/(moles of starting product initially present). Selectivity is defined as (moles of desired product formed)/(moles of starting product converted).

Decomposition of H_2O_2. Reactions were conducted with 0.15 g catalyst and 0.25 M H_2O_2 in 10 mL of MeOH. H_2O_2 was determined by cerimetry.[7]

EPR Detection of $O_2^{\bullet-}$, $OH^\bullet$, and $^1O_2$. Reactions were conducted with 3.75 mM catalyst and 0.8 M H_2O_2 in 1.5 mL MeOH. For $O_2^{\bullet-}$ detection, reaction suspensions were quickly frozen at 130 K after 10 min of reaction. For $^1O_2$ trapping, TEMP was added to the reaction in a 50 mM concentration; after 30 min, the suspension was centrifuged and the spectrum of the supernatant was recorded at room temperature in a flat quartz cell. Radicals were trapped by adding 0.1 M *N-tert*-butyl-α-phenylnitrone (PtBN) to the reaction; after 30 min, 4 g of water and 2 g of toluene were added to extract the adducts into the toluene layer. Spectra were recorded at room temperature in standard cylindrical EPR tubes.

Peroxidation of α-Terpinene. The reaction was run with 62.5 mM α-terpinene, 2.5 mM Mo or W, and 330 mM H_2O_2 in 4 mL MeOH, or on a larger scale, with 75 mM α-terpinene, 2.8 mM Mo, and 230 mM H_2O_2 (450 μL) in 20 mL MeOH. After 2.5 h, when the suspension had changed color from red to yellow, another portion of 450 μL of H_2O_2 was added. After consumption of a third portion of H_2O_2, α-terpinene was converted for over 99.5%. The product was isolated by addition of 50 mL water, followed by three extractions with 50 mL diethyl ether. The collected extracts were washed with 20 mL H_2O and dried over Na_2SO_4, yielding an oil with following ^{13}C NMR lines (CD_3OD): δ 138.0, 134.5, 81.7, 76.1, 33.9, 30.9, 27.1, 22.1, 18.0, 17.9 ppm.[8]

Formation of Other Endoperoxides. Rubrene: 1 mM rubrene, 0.225 mM Mo or W catalyst, 39 mM H_2O_2, 100 mL dioxane. 1,3-Diphenylisobenzofuran (DPIBF): 0.82 mM substrate, 0.6 mM catalyst, 29 mM H_2O_2, 100 mL THF. 1,4-Dimethylnaphthalene (DMN; reaction in a thermostatic bath at 20 °C): 42.7 mM DMN, 22.5 mM catalyst, 1.5 M H_2O_2 (added in three portions), 10 mL MeOH. For spectrophotometry, samples were sufficiently diluted with the organic solvent and quickly centrifuged. After completion of the reaction, white reaction products were isolated from the reactions with rubrene and DPIBF, by addition of 100 mL water and extraction into $CHCl_3$ (50 mL). Endoperoxide of rubrene: characteristic ^{13}C resonance at 84.7 ppm (C−O).[9] 1,2-Dibenzoyl benzene (from DPIBF): ^{13}C δ 196.7, 140.8, 138.1, 133.7, 131.3, 130.4, 130.3, 129.2 ppm.[10]

Hydroperoxidation of Olefins. Reactions were performed with 3 mmol olefin, 0.06 g of LDH catalyst, and 4 mL of MeOH (or 5 mL for 2,3,4-trimethyl-2-pentene and 1-methyl-1-cycloheptene). After 20 min of stirring, the reaction was started by addition of a portion of 1.65 mmol H_2O_2. Four subsequent portions of H_2O_2 were added with intervals of 1.5 h, for Mo, or 6 h, for W reactions. After complete H_2O_2 consumption, reaction mixtures were analyzed as such or after reduction of the hydroperoxides to the corresponding alcohols with tributylphosphine or Na_2SO_3.

Product distributions were determined with 0.1 M olefin, 2.8 mM catalyst, and 0.9 M H_2O_2 in MeOH. Competitive reactions were performed in identical conditions, with 0.05 M 2-methyl-2-pentene (MP) and 0.05 M of a second olefin A. Relative reactivities are given by

$$\frac{k_r^A}{k_r^{MP}} = \frac{\log(1 - [AO_2]_t/[A]_0)}{\log(1 - [MPO_2]_t/[MP]_0)} \quad (2)$$

with $[AO_2]_t$ and $[MPO_2]_t$ the concentrations at time t of the hydroperoxides formed from A and MP, and $[A]_0$ and $[MP]_0$ the initial olefin concentrations.[11]

Reference oxidations with H_2O_2/OCl^- were performed with solutions of olefin (0.1 M) and H_2O_2 (0.9 M) at 10 °C in 10 mL of MeOH. A 0.9 mL amount of 1.05 M NaOCl was added dropwise below the surface under vigorous stirring over 15 min. Prior to GC analysis, NaCl was removed by centrifugation.

The solvent deuterium effect was studied with 0.5 M cyclohexene, 1.87 mM catalyst, and 0.61 M H_2O_2 in 2 mL of MeOH or MeOH-d_4. Samples were taken after 5 h. Alternatively, 0.25 M 2,3-dimethyl-2-butene, 2.5 mM catalyst, and 0.29 M H_2O_2 were used; in this case, samples were taken after 1 h.

The effect of quenchers was studied with 0.375 M 2-methyl-2-pentene in 4 mL of MeOH, to which DABCO, NaN_3, or 2,6-di-*tert*-butylphenol was added (0−0.08 M). Reactions were started by addition of 2.5 mM catalyst and 0.55 M H_2O_2.

NIR Luminescence was detected from cuvettes with 3.8 mM catalyst and 450 mM H_2O_2 in 1.5 mL of MeOH or MeOH-d_4. As a reference, $^1O_2$ was generated photochemically with the sensitizer $Ru(bpy)_3^{2+}$. Emission spectra were recorded with an Edinburgh Instruments FL/FS 900 instrument, coupled to a liquid N_2 cooled Ge detector (North Coast EO-817). The light going to the detector was passed through a 110 Hz chopping wheel (Bentham 218). The detector signal was filtered by a muon filter (North Coast 829 B) and was processed by a lock-in amplifier (Bentham 225). For each sample, 10 scans were accumulated.

Instrumentation. For X-ray powder diffraction, a Siemens D5000matic with Ni-filtered Cu Kα radiation was used (40 kV, 50 mA). Infrared and Raman spectra were recorded with a Nicolet FT-IR 730 and a Bruker IFS200, respectively. Raman excitation was at 1062 nm (Nd:YAG, 50 mW); 28 scans were accumulated in 180° backscattering geometry. BET surface areas were obtained in an Coulter Omnisorp 100 CX apparatus from

TABLE 1: Physicochemical Characterization of the LDH Materials

	LDH−NO_3^-	LDH−MoO_4^{2-}	LDH−WO_4^{2-}
bulk analysis			
Mg/Al	2.30 (2.33)[a]	2.28	2.31
M/Al		0.056 (0.056)[b]	0.055
microanalysis[c]			
Mg/Al	2.25	2.23	2.28
M/Al		0.054	0.057
weight loss (%)			
in TGA			
<270 °C	11 (<180 °C)	14 (<220 °C)	14 (<215 °C)
>270 °C	37	29	30
cell dimensions (Å)			
a_0	3.045	3.048	3.044
c_0	24.52	24.20	24.26
layer charge density (e^+/Å^2)[d]	0.0393		
BET area (m^2 g^{-1})	92	87	88

[a] Theoretical value based on composition of LDH synthesis mixture. [b] Theoretical value based on amount of Na tungstate or molybdate used in the ion exchange. [c] Standard deviations (in %) for Mg, Al, Mo, and W were 2, 4, 8 and 9%, respectively. [d] $(2x)/(\sqrt{3}a_0^2)$ with x the Al^{3+} substitution in the formula $Mg_{1-x}Al_x(OH)_2[NO_3]_x \cdot zH_2O$.[50]

dynamic nitrogen adsorption at −196 °C. Prior to measurements, the lyophilized samples were heated in vacuo at 125 °C for 4 h. A Setaram TG-DTA92 was used for thermogravimetric analyses of LDHs (5 °C per minute, He) or rubrene endoperoxide (10 °C per minute, He/O_2). Particle size and morphology were determined with a Philips XL30 FEG scanning electron microscope (SEM). The bulk chemical composition was determined by atomic emission spectrometry on a Varian Liberty 100 apparatus with a plasma source (ICP). Samples were dissolved in 20% HNO_3 prior to analysis. Electron probe microanalysis (EPMA) was performed with a JEOL Microprobe JXA 733. ^{27}Al-MAS NMR spectra were recorded with a Bruker AMX-400 spectrometer with $Al(H_2O)_6^{3+}$ in water as a reference.

Reaction products were identified and quantified by GC or GC/MS, taking into account appropriate response factors. Liquid ^{13}C spectra were recorded with a Bruker AMX 300. For EPR, a Bruker ESP 300 was used with a rectangular TE_{104} cavity (9.5 GHz, 10 dB, 1 G modulation amplitude).

Results

Catalyst Characterization. An array of techniques was employed to thoroughly characterize the used LDH−NO_3^-, LDH−MoO_4^{2-}, and LDH−WO_4^{2-} catalysts. Some results are summarized in Table 1. Bulk chemical analysis (ICP) and microanalysis (EPMA) show practically the same Mg/Al ratio for the isolated solids as for the LDH precipitation mixture. The unit cell parameter a_0, as calculated from the [110] reflection in the X-ray diffractogram, is a measure for the mean cationic radius within the layers and therefore reflects the Mg/Al ratio.[12] The calculated value of 0.3045 nm is in full agreement with the $[Mg_{0.7}Al_{0.3}(OH)_2]^{0.3+}$ composition of the octahedral layer.[13] Contaminating phases, such as boehmite, were not detected by XRD. SEM pictures of the lyophilized LDH−NO_3^- material show large porous aggregates. These consist of small, hexagonal platelets, which are stacked co-facially or in a card-house type arrangement. The small crystallites have a diameter of 50−100 nm and are typically between 10 and 15 nm thick.

The Mo/Al and W/Al ratios of Table 1 (∼0.056) indicate that, at this low degree of ion exchange (11% of the total anion exchange capacity), the uptake of MoO_4^{2-} or WO_4^{2-} by the LDH−NO_3^- is essentially complete. After the ion exchange,

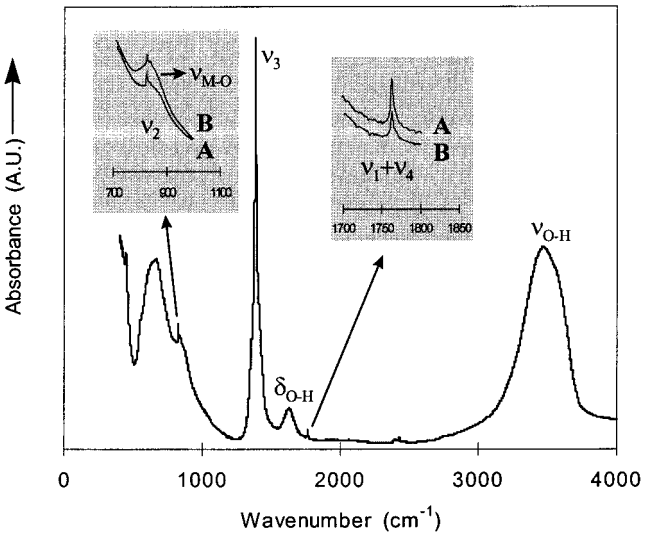

Figure 1. FTIR spectra of the precursor LDH−NO_3^- (A) and the oxometalate-exchanged LDH−MoO_4^{2-} (B).

EPMA analyses were performed on at least 30 arbitrarily chosen spots in the samples, and the results were subjected to a statistical analysis (Table 1). The small standard deviations for the Mg/Al, W/Al, and Mo/Al ratios prove that the exchanged anions are distributed homogeneously over the LDH samples.

Before as well as after ion exchange, the intergallery height in the LDH can be calculated from the position of the first basal [003] reflection around $2\theta = 11°$ ($c_0 = 3d_{(001)}$). Assuming 0.48 nm to be the thickness of the octahedral layer, the intergallery height is 0.35 nm for LDH−NO_3^-, which is smaller than the diameter of NO_3^- with D_{3h} symmetry (0.46 nm).[6] Ion exchange of WO_4^{2-} or MoO_4^{2-} for NO_3^- produces a slight intensity decrease for the basal reflections, but the c_0 values are practically unchanged. Moreover, the partial ion exchange does not affect the Mg/Al ratios, the a_0 parameter, nor the aspect of the material in SEM. The BET surfaces, as calculated from dynamic N_2 adsorption experiments, were only marginally lower for the oxometalate exchanged LDHs than for the initial nitrate form. There is no intragallery microporosity, not even after the ion exchange.

The presence of amorphous impurities was investigated with ^{27}Al-MAS NMR. Before and after ion exchange, the LDHs show a single sharp resonance at 9.4 ppm, attributed to Al^{3+} in 6-fold coordinated lattice positions.[14] This signal is much narrower than the octahedral signal of amorphous alumina (6 ppm); a signal of tetrahedral Al^{3+} (50−70 ppm) was not detected in the LDHs.[15]

With IR and Raman spectroscopy, the nature and speciation of the charge-compensating anions can be investigated. A well-resolved IR band is observed for NO_3^- at 1384 cm^{-1} (ν_3), with weaker, sharp bands at 827 (ν_2) and 1768 cm^{-1} ($\nu_1+\nu_4$) (Figure 1).[16] Upon ion exchange with the divalent oxometal anions, an additional broad IR absorption appears both for Mo and W LDHs near 820−850 cm^{-1}, assigned to the asymmetric M−O stretching vibration (ν_3).[16] Signals of the symmetrical ν_1 vibration (900−930 cm^{-1}) were not observed, indicating that the oxometalate ions are only weakly interacting with the support.

More information on the potential aggregation of oxo anions can be obtained from the Raman spectra (Figure 2).[17−20] A structural LDH band is observed at 555 cm^{-1}; NO_3^- has a strong symmetric stretching vibration (ν_1, 1055 cm^{-1}) and a weak in-plane bending vibration (ν_4, 719 cm^{-1}). Ion exchange with MoO_4^{2-} produces new bands at 894 ($\nu_{s,M=O}$) and 318 cm^{-1} ($\delta_{M=O}$); for LDH−WO_4^{2-}, bands appear at 937 ($\nu_{s,M=O}$) and

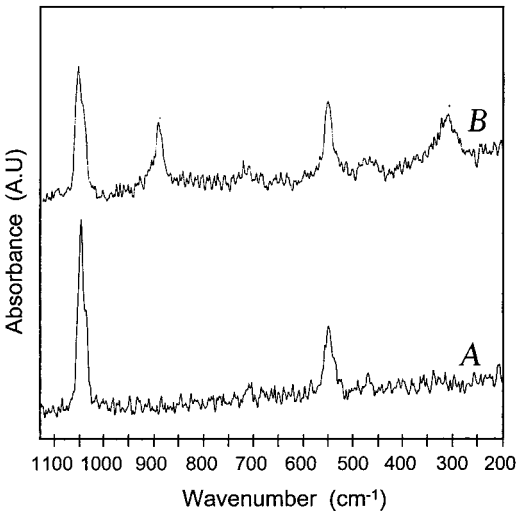

Figure 2. FT-Raman spectra of lyophilized LDH−NO_3^- (A) and LDH−MoO_4^{2-} (B).

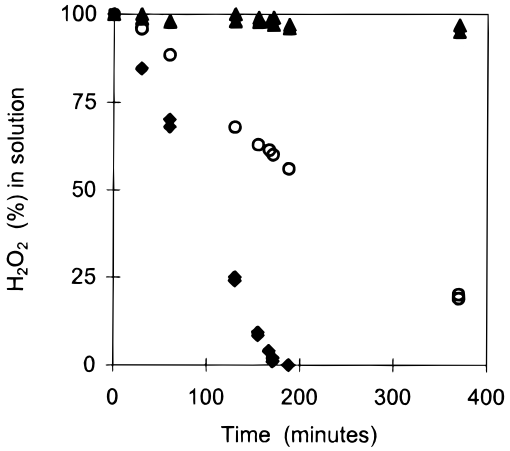

Figure 3. Disproportionation of H_2O_2 in the presence of LDH−NO_3^- (▲), LDH−WO_4^{2-} (○), and LDH−MoO_4^{2-} (◆) (0.15 g catalyst, 0.25 M H_2O_2, 10 mL MeOH).

342 cm^{-1} ($\delta_{M=O}$).[16] These frequencies were compared with literature data and our own observations for $(NH_4)_6Mo_7O_{24}\cdot 4H_2O$, $Mo_7O_{24}^{6-}$, $W_{12}O_{24}^{12-}$, $Na_2MoO_4\cdot 2H_2O$, MoO_4^{2-}, $Na_2WO_4\cdot 2H_2O$, and WO_4^{2-}.[18,19] This comparison convincingly demonstrates that the exchanged LDHs exclusively contain oxidic MO_4 species with tetrahedral T_d symmetry (M = Mo, W). The absence of a significant absorbance between 150 and 250 cm^{-1} shows that polymerized oxometalates with characteristic M−O−M deformation bands are not formed.[19] The monomeric character of the exchanged MoO_4^{2-} and WO_4^{2-} is in agreement with the relatively low degree of anion exchange, and with the well-known basic surface properties of the LDHs.[17,20]

Role of the LDH Support in the Decomposition of H_2O_2. As activation of H_2O_2 on basic LDHs has previously been described in the context of epoxidation, the contribution of the LDH support to the decomposition of H_2O_2 must be considered.[21,22] Figure 3 shows that the initial rates for peroxide decomposition in a MeOH suspension are 29, 11, and 0.8 μM s^{-1} for LDH−MoO_4^{2-}, LDH−WO_4^{2-}, and LDH−NO_3^- respectively. When these reactions are conducted in the presence of 2,3-dimethyl-2-butene (DMB, **1**) (see structures in Chart 1), the characteristic $^1O_2$ reaction product (2,3-dimethyl-3-hydroperoxo-1-butene, **2**) is detected for the LDH−MoO_4^{2-} and LDH−WO_4^{2-} catalysts, but not for LDH−NO_3^-. Consequently, it seems that the LDH support as such plays only a minor role in the decomposition of H_2O_2 or in the generation of $^1O_2$.

Semiquantitative Study of Reactive Oxygen Species (ROS) with EPR Spectroscopy. EPR measurements were performed on suspensions of LDH−MoO_4^{2-}, LDH−WO_4^{2-}, or LDH−NO_3^- in MeOH/H_2O_2 to detect short-lived oxygen species in a semiquantitative way. While detection of $^1O_2$ and $OH^\bullet$ requires addition of appropriate trapping agents, the superoxide anion $O_2^{\bullet-}$ can be observed directly by EPR.

LDH suspensions were exposed to H_2O_2 in the absence of any traps and, after 10 min at room temperature, quickly frozen down to 130 K. The LDH−NO_3^- suspension was completely EPR silent, while signals for molybdate- or tungstate-exchanged materials were extremely weak (parts a and b of Figure 4). Nevertheless, reference spectra of KO_2 suspended in MeOH, or of H_2O_2 in 1 M NaOH, show that the signal of free $O_2^{\bullet-}$ is easily detected (Figure 4c). Parameters are in agreement with the axial symmetry ($g_\perp = 2.023$; $g_\parallel = 2.092$).

To detect free $OH^\bullet$ radicals, 0.1 M *N-tert*-butyl-α-phenylnitrone (PtBN, **3**) was added to a suspension of the LDH in methanol/H_2O_2.[23,24] The addition of an alcohol solvent is required, as adducts of $OH^\bullet$ and PtBN are fairly unstable. However, $OH^\bullet$ radicals are known to produce α-hydroxyalkyl radicals by proton abstraction from alcohols. The adducts of these $^\bullet C(OH)R_2$ radicals and PtBN are stable and can be extracted with toluene:

$$OH^\bullet + CH_3OH \rightarrow {}^\bullet CH_2OH + H_2O \qquad (3)$$

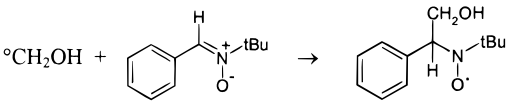

(4)

The validity of this "double trapping" method was checked for the decomposition of H_2O_2 by $FeSO_4\cdot 7H_2O$. This resulted in the observation of a strong six-line signal, due to the hyperfine coupling with ^{14}N and ^1H. The values for the hyperfine constants recorded in toluene ($a_N = 14.9$ G; $a_H = 3.1$ G) deviate only slightly from those reported in the literature, for RO−PtBN adducts dissolved in alcoholic solvents.[24] Such a signal was not observed at all with LDH−NO_3^-. With the oxometalate-exchanged LDHs, a very weak but clearly distinguishable six-line pattern was detected, indicating that a small amount of radical adducts has been formed (parts d and e of Figure 4). Remark that $^1O_2$ does not form spin adducts with PtBN.[25]

Finally, 2,2,6,6-tetramethylpiperidine (TEMP, **4**) was added to reaction suspensions as a trap for $^1O_2$. $^1O_2$ reacts with TEMP to form the stable nitroxide TEMPO **5** ($a_N = 16.3$ G).[26] With LDH−NO_3^-, no EPR signal was observed, but the signal intensity was substantial for LDH−WO_4^{2-} and LDH−MoO_4^{2-} (Figure 5). Quantification by double integration after identical reaction times shows that LDH−MoO_4^{2-} produces TEMPO 3−4 times faster than LDH−WO_4^{2-}.

Formation of Endoperoxides. Several dienes and conjugated aromatic compounds react with $^1O_2$ to form 1,4-endoperoxides. As there are not many alternative reaction mechanisms leading to these endoperoxides, the identification of an endoperoxide can contribute to prove the production of $^1O_2$.[1,8] Results are summarized in Table 2 and Figures 6 and 7. With LDH−MoO_4^{2-} and α-terpinene **6**, the conversion of the substrate is 92% after 3 h, with a selectivity for the endoperoxide (ascaridol, **7**) of 90% (Table 2). With LDH−WO_4^{2-}, the conversion of the substrate is much slower and, additionally, the selectivity for the endoperoxide is lower (51%). An important

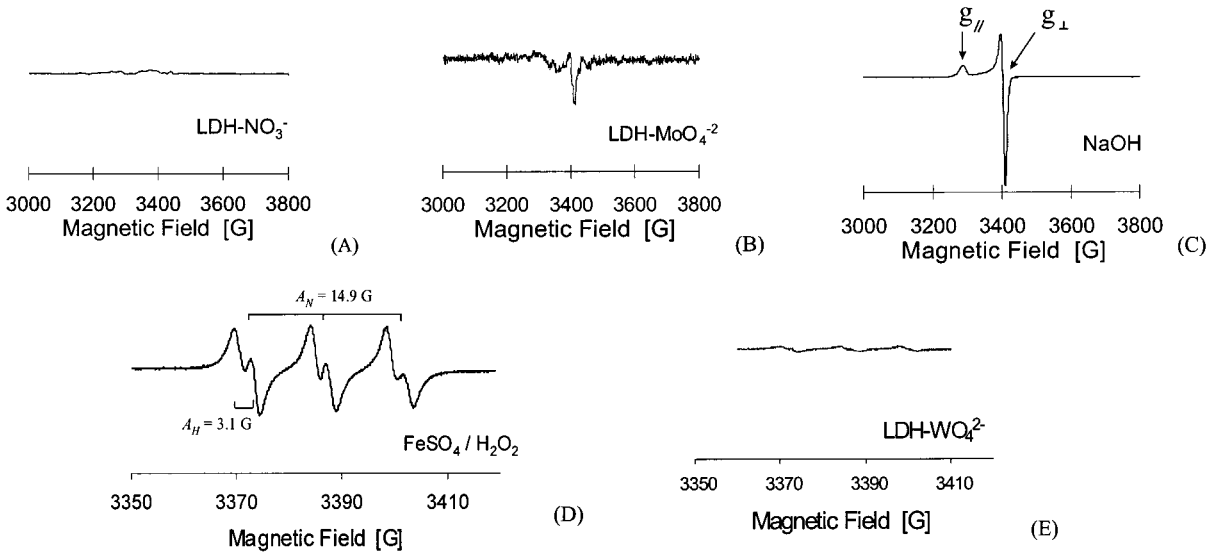

Figure 4. EPR detection of $O_2^{\bullet-}$ (A−C) and $OH^{\bullet}$ (D and E): (A) LDH−NO_3^- + H_2O_2 in MeOH, frozen at 130 K; (B) LDH−MoO_4^{2-} + H_2O_2 in MeOH, 130 K; (C) spectrum of $O_2^{\bullet-}$, 0.9 M H_2O_2, 1 M NaOH, 130 K; (D) $^{\bullet}CH_2OH$ adduct of PtBN, formed in Fe-catalyzed H_2O_2 decomposition (toluene, room temperature); (E) trapping of $^{\bullet}CH_2OH$ radicals in the reaction of H_2O_2 and LDH−WO_4^{2-} in MeOH.

CHART 1

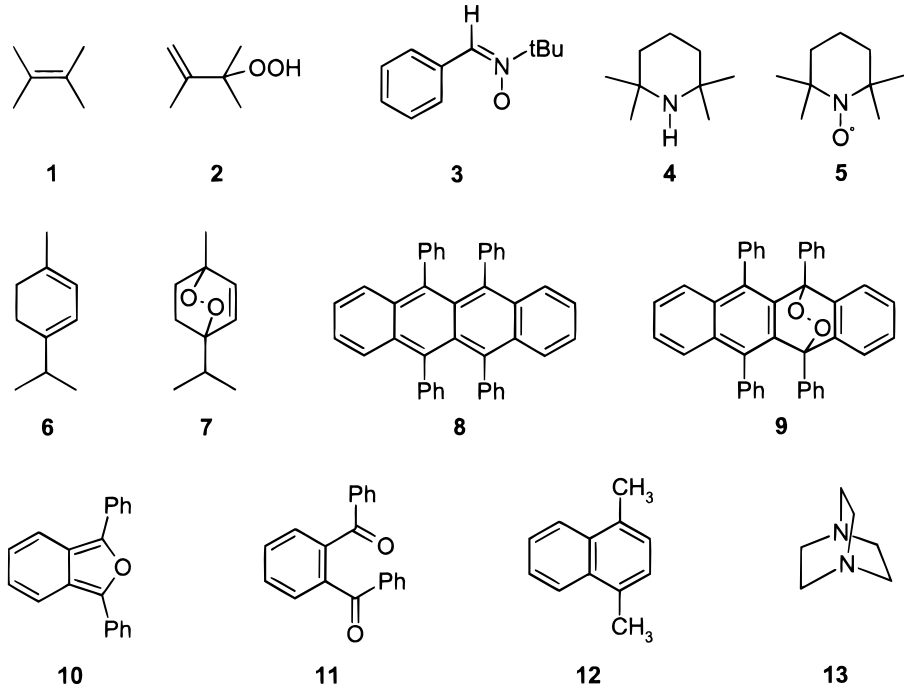

side reaction is the formation of the monoepoxides of α-terpinene. No endoperoxide is obtained with LDH−NO_3^- alone. Note that the same order of activity (Mo > W) is observed when dissolved molybdate and tungstate salts are used instead of the heterogeneous catalyst. The activity of the heterogeneous catalysts per mole of Mo or W is similar or even higher than for the homogeneous catalysts. By monitoring the catalytic activity of the supernatant of the heterogeneous reactions, it has been ascertained that 99.5% or more of the active Mo or W remains on the LDH support during the reaction.

The LDH−MoO_4^{2-} and LDH−WO_4^{2-} catalysts were also successfully used in the peroxidation of rubrene (**8**), 1,3-diphenylisobenzofuran (**10**), and 1,4-dimethylnaphthalene (**12**, DMN). The bleaching of these colored compounds is easily followed with UV−vis spectroscopy (Figure 6). Note that the spectrophotometry is much simplified by the heterogeneous character of the catalyst, which can be temporarily removed by a short centrifugation; with, e.g., dissolved sensitizers, spectral overlap is often a major problem. Reactions with the Mo catalyst were generally 4 or 5 times faster than with the W catalyst. In the case of 1,3-diphenylisobenzofuran, the endoperoxide is unstable and rearranges into 1,2-dibenzoylbenzene (**11**).[10] The identity of the reaction products was confirmed by several methods. First, endoperoxides were prepared with a known $^1O_2$ source, such as the Kasha−Khan reaction (OCl^- + H_2O_2), and characteristics of the product, e.g., GC retention time for ascaridol, were compared with those of the product of the LDH reaction. Alternatively, products were isolated and characterized by ^1H and ^{13}C NMR spectra. Finally, a characteristic test is the thermal decomposition of the endoperoxides.[2a,27] Thus, solid rubrene endoperoxide **9** decomposes upon heating to 170−195 °C with regeneration of the red rubrene; a solution of the endoperoxide of DMN almost fully reforms DMN when heated for 1 h at 60 °C (Figure 7). Note that, because of this thermal

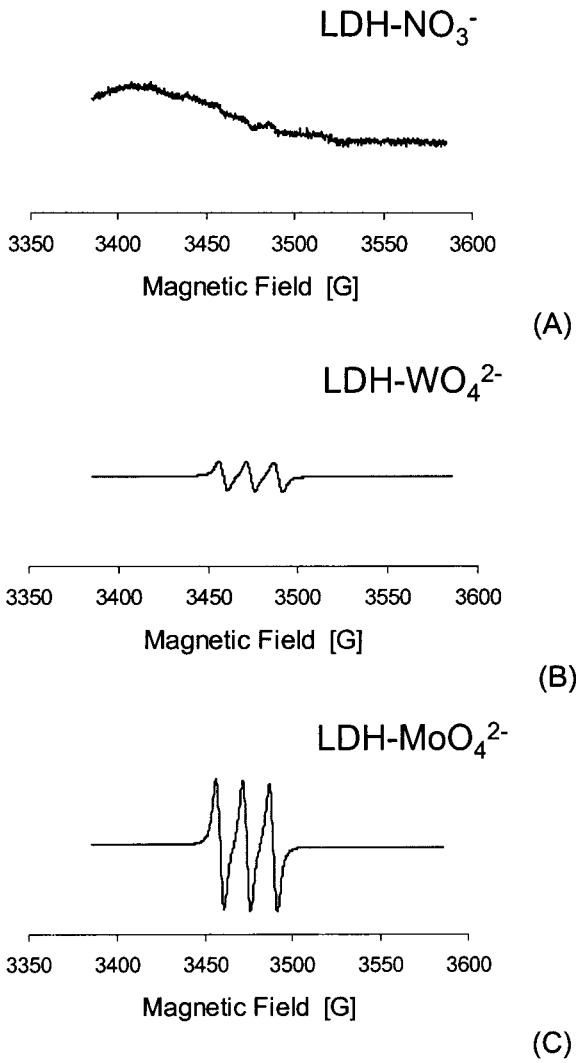

Figure 5. EPR spectra of TEMPO formed in catalyzed H_2O_2 disproportionation: (A) LDH−NO_3^-, (B) LDH−WO_4^{2-}, and (C) LDH−MoO_4^{2-}.

lability, the peroxidation of DMN did not succeed with the less active LDH−WO_4^{2-} catalyst. Apparently, the regeneration of the aromatic compound is even at 20 °C too fast in comparison with the peroxidation.

H_2O_2 Decomposition in the Presence of Olefins. *a. Olefin Reactivities and Product Selectivities.* $^1O_2$ converts olefins with at least one allylic hydrogen atom into hydroperoxides via the Schenck reaction, which involves H abstraction and migration of the double bond to an adjacent position in the carbon skeleton.[28,29] Hydroperoxide yields and selectivities are reported in Table 3 for reactions catalyzed by LDH−MoO_4^{2-} and LDH−WO_4^{2-}. For all reactions, results are given at complete consumption of H_2O_2. The olefins are ordered in Table 3 according to decreasing hydroperoxide yield in the reactions with LDH−MoO_4^{2-}. In these reactions, the hydroperoxide selectivity is over 95%, except for the least reactive substrate, cyclohexene. As $^1O_2$ is subject to solvent quenching, the susceptibility of an olefin to $^1O_2$ reaction is most conveniently derived from its Foote index β, i.e., the olefin concentration required to trap exactly half of the $^1O_2$ in solution.[30] Hence, a larger $1/\beta$ value means an easier reaction with $^1O_2$. Note that, for the Mo catalyst, the hydroperoxide yields of Table 3 exactly follow the same order as the reported $1/\beta$ values.

With LDH−WO_4^{2-}, the hydroperoxide selectivities are generally lower than for LDH−MoO_4^{2-}, due to a competing epoxidation. The hydroperoxide yield order of the olefins is the same as with LDH−MoO_4^{2-}, except for 2,3-dimethyl-2-butene, for which the epoxide selectivity is relatively large (47%).

Relative hydroperoxidation rates of olefins were determined in competitive experiments, with 2-methyl-2-pentene as a reference (Table 3, columns 5−9). For the sake of comparison, these reactivity ratios were also determined for some known $^1O_2$ sources (dissolved MoO_4^{2-} + H_2O_2 or OCl^-/H_2O_2) or were compiled from literature for a photosensitized reaction.[30] The ratios for the LDH−MoO_4^{2-} and LDH−WO_4^{2-} catalysts closely match those of the reported $^1O_2$ sources, particularly when one considers the large spread of hydroperoxidation rates (∼10 000).

Finally, isomer distributions within the hydroperoxide fraction were used as fingerprints of $^1O_2$.[29,31] Distributions are given in Table 4 for the reactions with the W and Mo LDH catalysts. Comparison with the isomer patterns obtained in other $^1O_2$ reactions reveals an excellent agreement. For 1-methyl-1-cyclohexene, the fraction of hydroperoxide B is particularly interesting.[32] This product may also be formed in a free radical allylic peroxidation. However, as the isomer distributions for the LDH reactions are the same as those for the authentic $^1O_2$ reactions, free radical reactions do not significantly contribute to product formation with the LDHs.

b. Effect of Solvent Deuteration on the Hydroperoxidation. As the lifetime of $^1O_2$ can be strongly lowered by the presence of hydrogen atoms in the solvent, deuteration of the solvent may increase the yield of the Schenck hydroperoxidation.[33] These effects are particularly expected when the olefin concentration is well below the β value; in that case, the major part of $^1O_2$ is lost by collision with the solvent. For the reaction of 0.5 M cyclohexene in methanol (β = 26 M),[30] the initial hydroperoxidation rate with LDH−MoO_4^{2-} is 6 times higher when CD_3OD is used as a solvent instead of CH_3OH.

The same experiment was performed with 0.25 M 2,3-dimethyl-2-butene. In the protonated as well as in the deuterated reaction medium, the final hydroperoxide yields are the same. This indicates that all $^1O_2$ available in solution is efficiently trapped by the olefin, as can be expected based on the very low β value (β = 0.3 mM).[30] However, the initial hydroperoxidation rate was 1.25 times *lower* in CD_3OD than in CH_3OH.

c. Effect of Quenchers on the Olefin Hydroperoxidation. Addition of the radical trap 2,6-di-*tert*-butylphenol (0.062 M) does not affect the hydroperoxide yields in the reaction of 2-methyl-2-pentene with H_2O_2 and the LDH−MoO_4^{2-} or LDH−WO_4^{2-} catalysts. However, addition of particularly DABCO (1,4-diazabicyclo[2.2.2]octane **13**) or NaN_3 decreases the hydroperoxide yield.[34,35] If this is caused by physical quenching of $^1O_2$, the variation of the hydroperoxide yield after identical reaction times with quencher concentration may be described by the following equation:[36]

$$\frac{[MPO_2]_0}{[MPO_2]_Q} = 1 + \frac{k_Q[Q]}{k_d + k_r^{MP}[MP]} \qquad (5)$$

with $[MPO_2]_0$ and $[MPO_2]_Q$ the hydroperoxide concentrations in the absence and in the presence of a quencher Q; k_d is the pseudo first-order rate constant for $^1O_2$ decay in methanol (1.1×10^5 s^{-1}); k_r^{MP} is the bimolecular rate constant for hydroperoxidation of 2-methyl-2-pentene (7×10^5 M^{-1} s^{-1}) and k_Q is the bimolecular rate constant for physical quenching of $^1O_2$ (1.2×10^7 M^{-1} s^{-1} for DABCO; 2.2×10^8 M^{-1} s^{-1} for N_3^-).[30] Plots of $[MPO_2]_0/[MPO_2]_Q$ vs [DABCO] or $[N_3^-]$ are given in Figure 8. As the concentration of 2-methyl-2-pentene (0.375

TABLE 2: Peroxidation of α-Terpinene (62.5 mM) with H_2O_2 (0.33 M) and Heterogeneous or Homogeneous Catalysts

	LDH−MoO_4^{2-}	LDH−WO_4^{2-}	LDH−NO_3^-	MoO_4^{2-}	WO_4^{2-}
time (h)	3	15	8	4.5	18
ascaridol yield (%)	83	40	0	91	54
ascaridol selectivity (%)	90	51		93	68

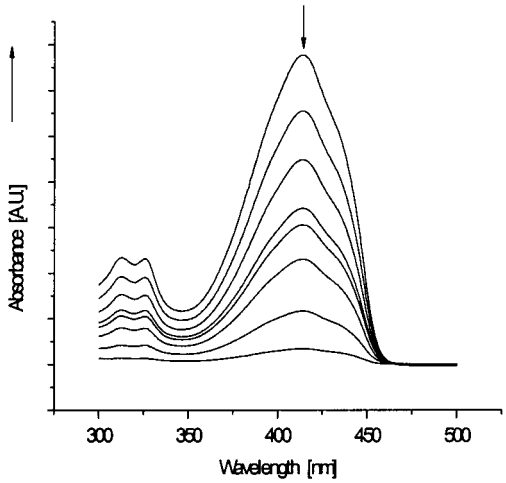

Figure 6. Bleaching of 1,3-diphenylisobenzofuran (0.82 mM) by LDH−MoO_4^{2-} and H_2O_2. UV−vis spectra were recorded after (from top to bottom) 0, 11, 23, 45, 52, 70, 110, and 160 min.

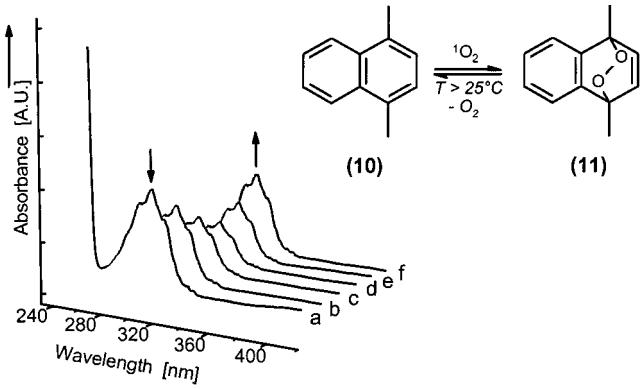

Figure 7. Endoperoxide formation from 1,4-dimethylnaphthalene in the presence of LDH−MoO_4^{2-}/H_2O_2: (a) initial spectrum; (b) after addition of 600 μL 35% H_2O_2 and 40 min reaction; (c and d) after one and two new additions of 600 μL H_2O_2; next, the sample is centrifuged and the supernatant is heated at 60 °C for 10 min (e) or 60 min (f).

M) is fairly large and hardly changes in the experiment, plots should be linear. For the reaction of 2-methyl-2-pentene with LDH−MoO_4^{2-} in the presence of DABCO, a linear plot is obtained with a slope of 19 M^{-1}; based on literature values for the rate constants, a value of 32 M^{-1} would be predicted. With LDH−MoO_4^{2-} and N_3^-, a linear plot is observed, but the slope (3.6 M^{-1}) is about 2 orders of magnitude smaller than that calculated from literature values (480 M^{-1}).[37] Moreover, it was noticed that the H_2O_2 disproportionation rate was strongly increased in the presence of azide and unusual byproducts showed up in the GC chromatograms. Finally, with LDH−WO_4^{2-} and DABCO, the slope is much lower than expected and a considerable deviation from linearity is observed. Remarkably, not only the hydroperoxide yield but also the epoxide yield (cfr. Table 3) was considerably decreased in the presence of DABCO; moreover, chromatography indicates that DABCO is gradually consumed during the reaction with LDH−WO_4^{2-}, while there was no such consumption with LDH−MoO_4^{2-}.

Direct Observation of $^1O_2$ via NIR Luminescence. With a highly sensitive liquid N_2 cooled Ge detector, $^1O_2$ may be observed directly, due to the $^1\Delta_g \rightarrow {}^3\Sigma_g^-$ monomol decay at 1268 nm (Figure 9).[3,38] For the decomposition of H_2O_2 in the presence of LDH−MoO_4^{2-}, the emission intensity is about 8 times stronger in CD_3OD than in CH_3OH. With LDH−WO_4^{2-} in CD_3OD, the emission is about 4 times weaker than with LDH−MoO_4^{2-} in the same solvent, indicating that the rate of $^1O_2$ production is considerably smaller with W than with Mo. In both cases, the emission intensity was constant over at least 40 min.

Discussion

Catalyst Characterization. Within the detection limits of the techniques used, the LDHs are free of crystalline or amorphous impurities and possess a high degree of compositional homogeneity. The exchanged Mo or W is present as free, monomeric molybdate or tungstate, withheld electrostatically by the positively charged octahedral layers. No evidence has been found, e.g., in the ^{27}Al NMR or the vibrational data, for the existence of the surface-grafted or oligomerized species that are formed in phosphate-, silicate-, or vanadate-containing LDHs.[14,39] Note that the conditions for synthesis of LDHs with polymerized tungstate or molybdate pillars are quite different, e.g., pH control at 4.5 with 4 N HNO_3, higher oxometalate concentrations (up to 0.4 M), or use of preformed solutions of polyoxoanions.[40] Hence, the present materials, with exchanged, monomeric MO_4^{2-} are substantially different from the $H_2W_{12}O_{40}^{6-}$ or $Mo_7O_{24}^{6-}$ pillared materials which have been used as epoxidation catalysts.[6,40]

As the gallery height, the XRD pattern, the porosity, and the SEM picture are hardly changed by the MO_4^{2-} exchange, it seems unlikely that the MO_4^{2-} anions enter the intragallery space to a considerable extent. Rather, in view of the high layer charge density and the large external surface, and because of the low exchange degree, a large fraction of the MO_4^{2-} anions may be located on edge sites and at the external surface. Except for the nature of the oxometal anion (MoO_4^{2-} or WO_4^{2-}), the LDH−MoO_4^{2-} and LDH−WO_4^{2-} catalysts seem to have highly similar physical properties, such as surface area, metal content, or gallery height. Hence, any differences between the two catalysts in H_2O_2 consumption or $^1O_2$ production rates should primarily be related to the nature of the exchanged anion.

Methods for $^1O_2$ Detection. Literature contains a multitude of more or less reliable methods for the detection of $^1O_2$. The major part of these tests has been developed for $^1O_2$ generation by dissolved dye sensitizers. The results for the LDH−MoO_4^{2-} or LDH−WO_4^{2-} catalyzed decomposition of H_2O_2 into $^1O_2$ enable the limitations or potential errors inherent to these methods to be fully appreciated.

The solvent isotope effect observed in the hydroperoxidation of cyclohexene ($\upsilon_{CD3OD}/\upsilon_{CH3OH} = 6$) is caused by the longer lifetime of $^1O_2$ in CD_3OD ($k_d = 4.4 \times 10^3\ s^{-1}$) than in CH_3OH ($k_d = 1.08 \times 10^5\ s^{-1}$).[30] However, the isotopic purity is not complete, and this complicates the calculation of expected isotope effects. Taking into account the volume fractions of water (5%; $k_d = 2 \times 10^5\ s^{-1}$) and olefin (4.5%; $k_d = 4 \times 10^4\ s^{-1}$), one would expect an isotope effect of 7.6, instead of the

TABLE 3: Hydroperoxide Yields and Selectivities in the Reaction of Various Olefins with H_2O_2 in MeOH in the Presence of LDH−MO_4^{2-} (M = Mo and W)[a]

Substrate	1 / β [30]	Yield (Selectivity) LDH-WO_4^{2-}	Yield (Selectivity) LDH-MoO_4^{2-}	Relative Reactivity LDH-WO_4^{2-}	Relative Reactivity LDH-MoO_4^{2-}	Relative Reactivity MoO_4^{2-} / H_2O_2	Relative Reactivity Sens / *hν* [30]	Relative Reactivity OCl^- / H_2O_2
	333	46 (53)	87 (98)	34	29	32	52	45
	200	65 (75)	80 (98)	22	19	22	20	19
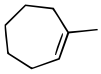	14.3	38 (51)	73 (96)	0.32	0.35	0.36	0.39	0.39
	9.1	26 (37)	61 (98)	1.5	1.5	1.4	1.3	1.3
	9.1	25 (31)	60 (97)	1.6	1.5	1.6	2.6	1.4
	5.5	19 (23)	58 (96)	1	1	1	1	1
	1.4	19 (30)	45 (98)	0.17	0.16	0.16	0.22	0.25
	1	8 (11)	27 (95)	0.08	0.06	0.055	0.18	0.06
	0.018	3 (5)	3 (70)	0.009	0.007	0.005	0.003	0.006

[a] Relative reactivities are determined with 2-Me-2-pentene as a reference.

TABLE 4: Product Distribution (for the Hydroperoxide Fraction) of the Reaction of Various Olefins with H_2O_2 in MeOH in the Presence of LDH−MO_4^{2-}

Entry	Substrate	Hydro-peroxide A	Hydro-peroxide B	Hydro-peroxide C	OCl^- / H_2O_2 A	OCl^- / H_2O_2 B	OCl^- / H_2O_2 C	Photo-oxygenation [30] A	Photo-oxygenation [30] B	Photo-oxygenation [30] C	MoO_4^{2-} / H_2O_2 A	MoO_4^{2-} / H_2O_2 B	MoO_4^{2-} / H_2O_2 C	LDH-MoO_4^{2-} / H_2O_2 A	LDH-MoO_4^{2-} / H_2O_2 B	LDH-MoO_4^{2-} / H_2O_2 C	LDH-WO_4^{2-} / H_2O_2 A	LDH-WO_4^{2-} / H_2O_2 B	LDH-WO_4^{2-} / H_2O_2 C
1					100			100			100			100			100		
2					51	49		52	48		48	52		52	48		51	49	
3		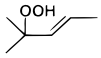			49	51		51	49		47	53		47	53		48	52	
4					39	61	0	40	60	0	41	59	0	42	58	0	43	57	0
5			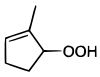		4	40	56	4	43	53	4	43	53	4	42	54	4	43	53
6					44	20	36	44	20	36	44	15	39	43	16	41	40	19	40
7								4	48	48	4	49	47	5	50	45	5	47	48

observed value of 6. For the luminescence experiment, a similar difference between the expected (9.2) and real value (8) is observed. Such discrepancies are not unusual. First, the used catalyst is in the H form, and its surface is covered with potentially quenching anions. This contributes to an unknown extent of the overall quenching process.[41] Second, the estimates do not consider a possible solvent dependence of the rate constants, e.g., for reaction with the substrate.[2a] Third, the experiment with 2,3-dimethyl-2-butene suggests that, even if the total hydroperoxide yield is the same in CD_3OD and CH_3OH, the generation of $^1O_2$ is appreciably slower in CD_3OD than in CH_3OH. Summarizing, solvent effects are more

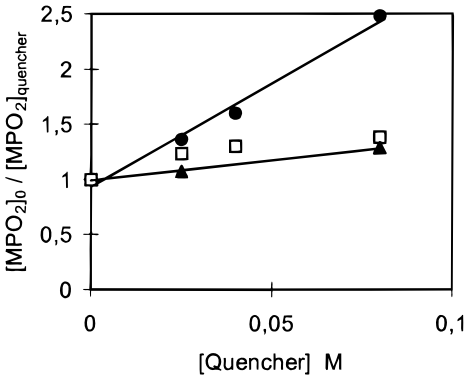

Figure 8. Effect of the quenchers DABCO and N_3^- on the hydroperoxidation of 2-methyl-2-pentene (0.375 M): $[MPO_2]_{quencher}$ = hydroperoxide concentration in the presence of quencher; $[MPO_2]_0$ = hydroperoxide concentration without quencher; (●) LDH−MoO_4^{2-}, DABCO, 1 h; (□) LDH−WO_4^{2-}, DABCO, 9 h; (▲) LDH−MoO_4^{2-}, NaN_3, 1 h.

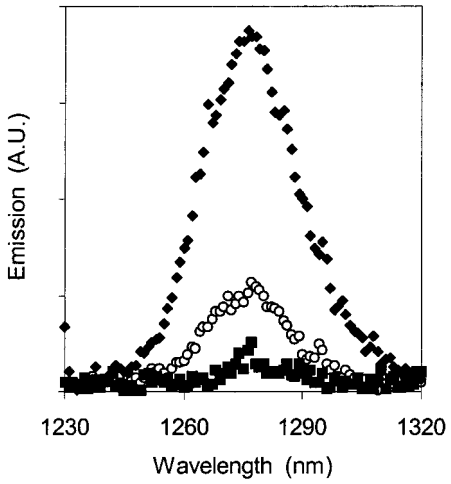

Figure 9. Chemiluminescence of $^1O_2$ in the LDH catalyzed disproportionation of H_2O_2: LDH−MoO_4^{2-} in MeOH (■) and MeOH-d_4 (◆); LDH−WO_4^{2-} in MeOH-d_4 (○).

ambiguous to interpret than one would expect based on the large lifetime differences. Even other reactive oxygen species, such as the superoxide anion, display solvent isotope effects, albeit smaller than those for $^1O_2$.[42]

Endoperoxide formation is a characteristic reaction for $^1O_2$.[27] However, with less reactive aromatic compounds such as 1,4-dimethylnaphthalene, the rate of $^1O_2$ formation must be sufficiently high to compensate for the thermal decomposition of the endoperoxide. Consequently, for the rather slow reaction with the LDH−WO_4^{2-} catalyst, one fails to observe endoperoxide formation from 1,4-dimethylnaphthalene, and with LDH−MoO_4^{2-}, a large catalyst concentration is required (Figure 7). It should also be noted that endoperoxides may be formed via alternative routes, e.g. by reaction of $^3O_2$ with the cation radical of α-terpinene.[43]

The physical quenching experiment with DABCO succeeded with LDH−MoO_4^{2-}, but failed with W because of direct oxygenation of DABCO (Figure 8). This not only reduces the amount of N free electron pairs which are the active quenchers but also implies that less peroxide is available for $^1O_2$ generation. Even more complications arise with the azide trapping agent. The accelerated H_2O_2 disproportionation and the side products suggest that N_3^- induces radical chain side reactions, e.g., via the known reduction of $^1O_2$ by N_3^- to $O_2^{\bullet-}$.[35] Concomitantly, the $N_3^\bullet$ radicals formed may give rise to azide−olefin adducts. Moreover, ion exchange of the azide on the LDH might decrease the availability of N_3^- in the bulk of the solution and hence its capability of quenching freely diffusing $^1O_2$.[44,45] Finally, the EPR method with TEMP as a $^1O_2$ trap should not be used if the catalyst is suspected to be capable of mono-oxygen transfer (Figure 5). With LDH−WO_4^{2-}, the TEMPO may be formed in a reaction with $^1O_2$; however, the TEMP might also be oxidized by oxygen transfer from peroxo-W complexes, first to the hydroxylamine, and next to the hydroxylamine *N*-oxide. The latter is known to decompose homolytically to $OH^\bullet$ radicals and TEMPO. [46]

The foregoing discussion implies that, of all $^1O_2$ tests, $^1O_2$ luminescence in the NIR (Figure 9) and correct hydroperoxide isomer distributions from olefins constitute the most reliable proofs for involvement of $^1O_2$. For LDH−WO_4^{2-}, the hydroperoxide patterns of Table 4 are particularly convincing.

Evidently, $^1O_2$ observation never excludes the presence of other active oxygen species. First, in combination with H_2O_2, LDH−WO_4^{2-} is capable of transferring a single oxygen atom, which probably originates in a peroxo−W compound. This causes the appreciable epoxide selectivities in the reactions with olefins (Table 3).[47] Moreover, such mono-oxygen transfer is also possible with amines, and this jeopardizes tests involving the amines DABCO and TEMP.[48] With LDH−MoO_4^{2-}, mono-oxygen transfer is almost negligible. This is consistent with results for homogeneous Mo catalysts, which only effect epoxidation when the pH is sufficiently low to cause oligomerization of the Mo. With monomeric molybdate, as in the LDH−MoO_4^{2-} catalyst, singlet oxygen production predominates.[49] For LDH−WO_4^{2-} and for LDH−MoO_4^{2-}, a small amount of free radicals is detected with the EPR double trapping method (Figure 4). However, these radicals do not significantly contribute to olefin oxygenations, as demonstrated by the isomer patterns of Table 4, and by the ineffectiveness of the phenol radical trap.

Summarizing, the LDH−MoO_4^{2-} is a performant heterogeneous catalyst for $^1O_2$ generation, with minimal interference by nondesired reactive oxygen species. The related W catalyst produces $^1O_2$ at a considerably slower rate, and this reaction should be considered if LDH−WO_4^{2-} is to be used as a heterogeneous catalyst for selective mono-oxygenation of for instance olefins.[47]

Acknowledgment. We are indebted to IWT (B.F.S.) and FWO (D.E.D.V. and P.J.G.) for research positions. This project was sponsored by the Belgian Government in the frame of an I.U.A.P. project *Supramolecular Catalysis*. We thank F. Pelgrims for SEM and EPMA measurements, Prof. T. Zeegers for use of the Raman spectrometer, and B. Wouters for recording the Al-NMR spectra.

References and Notes

(1) (a) *Singlet Oxygen*; Frimer, A. A., Ed.; CRC Press: Boca Raton, FL, 1985; Vols. 1−4. (b) Clennan, E. L. *Tetrahedron* **1991**, *47*, 1343.

(2) (a) Aubry, J. M. *J. Am. Chem. Soc.* **1985**, *107*, 5844. (b) Aubry, J. M.; Cazin, B. *Inorg. Chem.* **1988**, *27*, 2013. (c) Nardello, V.; Marko, J.; Vermeersch, G.; Aubry, J. M. *Inorg. Chem.* **1995**, *34*, 4950. (d) Aubry, J. M.; Bouttemy, S. *J. Am. Chem. Soc.* **1997**, *119*, 5286.

(3) Böhme, K.; Brauer, H.-D. *Inorg. Chem.* **1992**, *31*, 3468.

(4) van Laar, F.; De Vos, D. E.; Vanoppen, D.; Sels B. F.; Jacobs P. A.; Del Guerzo, A.; Pierard, F.; Kirsch-De Mesmaeker, A. *Chem. Commun.* **1998**, 267.

(5) (a) Trifirò, F.; Vaccari, A. In *Comprehensive Supramolecular Chemistry*; Alberti, G., Bein, T., Eds.; Pergamon: Elmsford, NY. 1996; Vol. VII. (b) Cavani, F.; Trifirò, F.; Vaccari, A. *Catal. Today* **1991**, *11*, 173 and references therein.

(6) Gardner, E.; Pinnavaia, T. J. *Appl. Catal. A* **1998**, *167*, 65.

(7) Vogel, A. I.; Bassett, J. *Vogel's Textbook of Quantitative Inorganic Analysis*; Longman: London, 1978.
(8) Okuyama, E.; Umeyama, K.; Saito, Y.; Yamazaki, M.; Satake, M. *Chem. Pharm. Bull.* **1993**, *41*, 1309.
(9) Aubry, J. M.; Rigaudy, J.; Cuong, N. K. *Photochem. Photobiol.* **1981**, *33*, 149.
(10) Pouchert, C.; Behnke, J. *The Aldrich Library of ^{13}C and ^{1}H FT NMR Spectra*; Aldrich Chemical Co.: Milwaukee, WI, 1993.
(11) Foote, C. S.; Wuesthoff, M. T.; Wexler, S.; Schenck, G. O.; Schulte-Elte, K.-H. *Tetrahedron* **1967**, *23*, 2583.
(12) Brindley, G. W.; Kikkawa, S. *Am. Mineral.* **1979**, *64*, 836.
(13) Miyata, S. *Clays Clay Mineral.* **1980**, *28*, 50.
(14) Depège, C.; El Metoui, F.; Forano, C.; de Roy, A.; Dupuis, J.; Besse, J.-P. *Chem. Mater.* **1996**, *8*, 952.
(15) Thevenot, F.; Szymanski, R.; Chaumette, P. *Clays Clay Mineral.* **1989**, *37*, 396.
(16) Nakamoto, K. *Infrared and Raman Spectra of Inorganic and Coordination Compounds*, 5th ed.; John Wiley & Sons: New York, 1997.
(17) Twu, J.; Dutta, P. K. *J. Phys. Chem.* **1989**, *93*, 7863.
(18) (a) Niemantsverdriet, J. W. *Spectroscopy in Catalysis*; VCH: New York, 1995. (b) Payen, E.; Grimblot, J.; Kasztelan, S. *J. Phys. Chem.* **1987**, *91*, 6642. (c) Stencel, J. M. *Raman Spectroscopy for Catalysis*; Van Nostrand Reinhold: New York, 1990.
(19) Jeziorowski, H.; Knözinger, H. *J. Phys. Chem.* **1979**, *83*, 1166.
(20) (a) Contescu, C.; Jagiello, J.; Schwarz, J. A. *J. Phys. Chem.* **1993**, *97*, 10152. (b) Constantino, V. R. L.; Pinnavaia, T. J. *Inorg. Chem.* **1995**, *34*, 883.
(21) Cativiela, C.; Figueras, F.; Fraile, J. M.; García, J. I.; Mayoral, J. A. *Tetrahedron Lett.* **1995**, *36*, 4125.
(22) Ueno, S.; Yamaguchi, K.; Yoshida, K.; Ebitani, K.; Kaneda, K. *Chem. Commun.* **1998**, 295.
(23) Niki, E.; Yokoi, S.; Tsuchiya, J.; Kamiya, Y. *J. Am. Chem. Soc.* **1983**, *105*, 1498.
(24) Sridhar, R.; Beaumont, P. C.; Powers, E. L. *J. Radioanal. Nucl. Chem.* **1986**, *101*, 227.
(25) Harbour, J. R.; Issler, S. L.; Hair, M. L. *J. Am. Chem. Soc.* **1980**, *102*, 7779.
(26) (a) Lion, Y.; Delmelle, M.; Van de Vorst, A. *Nature* **1976**, *263*, 442. (b) Kawanishi, S.; Inoue, S.; Yamamoto, K. *Biol. Trace Elem. Res.* **1989**, *21*, 367.
(27) (a) Wasserman, H. H.; Scheffer, R.; Cooper, J. L. *J. Am. Chem. Soc.* **1972**, *94*, 4991. (b) Turro, N. J.; Chow, M. F.; Rigaudy, J. *J. Am. Chem. Soc.* **1981,** *103*, 7218. (c) Aubry, J. M.; Cazin, B.; Duprat, F. *J. Org. Chem.* **1989**, *54*, 727.
(28) Gilbert, A.; Baggott, J. *Essentials of Molecular Photochemistry*; CRC Press: Boca Raton, 1991; p 501.
(29) Prein, M.; Adam; W. *Angew. Chem., Int. Ed. Engl.* **1996**, *35*, 447.
(30) Wilkinson, F.; Helman, W. P.; Ross, A. B. *J. Phys. Chem. Ref. Data* **1995**, *24*, 663.
(31) Foote, C. S. *Acc. Chem. Res.* **1968**, *1*, 104.
(32) Pettit, T. L.; Fox, M. A. *J. Phys. Chem.* **1986**, *90*, 1353.
(33) (a) Merkel, P. B.; Kearns, D. R. *J. Am. Chem. Soc.* **1972**, *94*, 7244. (b) Ogilby, P. R.; Foote, C. S. *J. Am. Chem. Soc.* **1983**, *105*, 3423.
(34) Monroe, B. M. *J. Phys. Chem.* **1977**, *81*, 1861.
(35) Lissi, E. A.; Encinas, M. V.; Lemp, E.; Rubio, M. A. *Chem. Rev.* **1993**, *93*, 699.
(36) Peters, J. W.; Bekowies, P. J.; Winer, A. M.; Pitts, J. N. *J. Am. Chem. Soc.* **1975**, *97*, 3299.
(37) Hasty, N.; Merkel, P. B.; Radlick, P.; Kearns, D. R. *Tetrahedron Lett.* **1972**, *1*, 49.
(38) (a) Khan, A. U.; Kasha, M. *J. Am. Chem. Soc.* **1966**, *88*, 1574. (b) Rodgers, M. A. J.; Snowden, P. T. *J. Am. Chem. Soc.* **1982**, *104*, 5541**.**
(39) (a) Hansen, H. C. B. *Proc. 10th Int. Clay Conf.* **1995**, 201. (b) Kwon, T.; Tsigdinos, G. A.; Pinnavaia, T. J. *J. Am. Chem. Soc.* **1988**, *110*, 3653.
(40) (a) Dredzon, M. A. *Inorg. Chem.* **1988**, *27*, 7**,** 4628. (b) Ulibarri, M.; Labajos, F. M.; Rives, V. *Inorg. Chem.* **1994**, *33*, 2592. (c) Dimotakis, E. D.; Pinnavaia, T. J. *Inorg. Chem.* **1990**, *29*, 2393. (d) Narita, E.; Kaviratna, P.; Pinnavaia, T. J. *Chem. Lett.* **1991**, 805.
(41) Iu, K. K.; Thomas, J. K. *J. Am. Chem. Soc.* **1990**, *112*, 3319.
(42) Bielski, B. H. J.; Saito, E. *J. Phys. Chem.* **1971**, *75*, 2263.
(43) Nelsen, S. F. *Acc. Chem. Res.* **1987**, *20*, 269.
(44) Rubio, M. A.; Mártire, D. O.; Braslavsky, S. E.; Lissi, E. A. *J. Photochem. Photobiol. A: Chem.* **1992**, *66*, 153.
(45) Lee, P. C.; Rodgers, M. A. J. *J. Phys. Chem.* **1984**, *88*, 4385.
(46) Murray, R. W.; Singh, M. *Tetrahedron Lett.* **1988**, *29*, 4677.
(47) Sels, B. F.; De Vos, D. E.; Jacobs, P. A. *Tetrahedron Lett.* **1996**, *37*, 8557.
(48) Sheldon, R. A.; Kochi, J. K. *Metal-Catalyzed Oxidations of Organic Compounds*; Academic Press: New York, 1981.
(49) Nardello, V.; Bouttemy, S.; Aubry, J. M. *J. Mol. Catal. A* **1997**, *117*, 439.
(50) Yun, S. K.; Pinnavaia, T. J. *Chem. Mater.* **1995**, *7*, 348.